

Original Article



Exploring *Phacellanthus Tubiflorus* Sieb. et Zucc. (Orobanchaceae) as a Novel Herbal Therapeutic: Efficacy and Mechanisms in Alzheimer's Disease

Cheng Chang^{1,2}, Wenjie Yu³, Yuguang Fan³, Fengkun Cai^{1,2}, Shen Lu², Jiao Jiao¹, Zhiguo Liu¹, Chenlu Wang^{4*}, Yujie Fu^{4*}

¹Key Laboratory of Forest Plant Ecology, Engineering Research Center of Forest Bio-preparation, Ministry of Education, The College of Chemistry, Chemical Engineering and Resource Utilization, Northeast Forestry University, Harbin 150040, China

²Jilin Provincial Joint Key Laboratory of Changbai Mountain Biocoenosis and Biodiversity, Changbai Mountain Academy of Sciences, Antu 133613, China

³Engineering Research Center of Tropical Medicine Innovation and Transformation of Ministry of Education, International Joint Research Center of Human-Machine Intelligent Collaborative for Tumor Precision Diagnosis and Treatment of Hainan Province, Hainan Provincial Key Laboratory of Research and Development on Tropical Herbs, School of Pharmacy, Hainan Medical University, Haikou 571199, China

⁴The College of Biological Sciences and Technology, Beijing Forestry University, Beijing 100083, China

*Corresponding Author: Yujie Fu, Chenlu Wang

Abstract:

Alzheimer's disease (AD) is a major public health concern due to its widespread prevalence and limited effective treatments, highlighting the urgent need for innovative therapies. This study explores the therapeutic potential of *Phacellanthus tubiflorus* Sieb. et Zucc. (*P. tubiflorus*), a traditional Chinese medicine, as a potential source of neuroprotective agents. Systematically phytochemical analysis, employing UPLC-Q-TOF/MS, identified 1,536 compounds within *P. tubiflorus* including a notable abundance of Magnoloside D, Acteoside, and Cordycepin. Network pharmacology analyses, integrated with molecular docking studies, predicted a convergence between *P. tubiflorus*-derived compounds and central regulators of AD pathophysiology, notably SRC proto-oncogene (SRC), Tumor necrosis factor (TNF), AKT Serine/Threonine Kinase 1 (AKT1), Interleukin 1 Beta (IL-1B), and Interleukin 6 (IL-6). Enrichment analyses further implicated these interactions in key biological processes and signaling pathways, including neuroactive ligand-receptor interaction, cAMP signaling pathway, PI3k-Akt signaling pathway, all of which are dysregulated in AD. Importantly, these *in silico* predictions were substantiated by *in vitro* experiments using an A β ₁₋₄₂-challenged SH-SY5Y cell model, demonstrating that Magnoloside D can attenuate neuroinflammatory responses and modulate post-translational phosphorylation. These findings provide mechanistic insights into the potential therapeutic effects of *P. tubiflorus* and highlights its promise as a novel avenue for AD intervention.

Keywords: *Phacellanthus tubiflorus*; Alzheimer's Disease; Network Pharmacology; Molecular docking; Neuroprotection

Introduction

Alzheimer's disease (AD) constitutes a devastating and increasingly prevalent neurodegenerative disorder characterized clinically by progressive cognitive decline and

neuropathological hallmarks, including extracellular amyloid-beta (A β) plaques and intracellular neurofibrillary tangles (NFTs) composed of hyperphosphorylated tau protein^[1].

The etiology of AD is complex and multifactorial, involving a dynamic interplay between genetic susceptibility, age-related cellular senescence, chronic neuroinflammation, oxidative stress, and neurotransmitter dysregulation, particularly within the cholinergic system^[2]. Current pharmacological interventions, primarily comprising cholinesterase inhibitors and NMDA receptor antagonists, afford only modest symptomatic relief and, critically, fail to address the underlying disease mechanisms or halt disease progression^[3-5]. Consequently, there is an urgent need to explore novel therapeutic methods with disease-modifying potential. In this context, herbal medicines, derived from a rich tradition of ethnobotanical knowledge, present a promising avenue for therapeutic discovery. Herb's multi-target potential is particularly advantageous in the context of AD's complex pathogenesis, as it allows for the simultaneous modulation of multiple disease pathways^[6-8]. Furthermore, herbal extracts often demonstrate a favorable safety profile compared to synthetic drugs, suggesting the potential suitability for long-term therapeutic application^[9, 10].

Phacellanthus tubiflorus Sieb. et Zucc., a holoparasitic plant in the Orobanchaceae family, has a long history of use in traditional Chinese medicine (TCM) for reinforcing the kidney and strengthen Yang associated with male sexual function enhancement and treating conditions like lumbago and weakness^[11]. In TCM theory, the kidney system stores the vital essence 'Jing' which is believed to generate 'Marrow', encompassing the brain and spinal cord. A strong kidney nourishes the brain, supporting cognitive function. Additionally, Previous studies on *P. tubiflorus* have demonstrated its anti-fatigue and immune-enhancing effects^[11], and our preliminary research suggests that it also possesses potentially neuroprotective properties. These findings, coupled with its traditional uses, highlight the potential of *P. tubiflorus* as a source of novel therapeutic agents for AD.

Recent breakthroughs in network pharmacology and molecular docking techniques have revolutionized drug discovery processes, particularly in understanding the complex interactions between bioactive compounds and biological targets^[12, 13]. Here, we elucidate the therapeutic potential of *P. tubiflorus* against AD by integrating network pharmacological analyses

of herb-compound-target-disease interactions with molecular simulations. Furthermore, pivotal *in silico* predications are validated through targeted *in vitro* assays, providing the mechanistic rationale for *P. tubiflorus* as a promising source of novel AD therapeutics.

2. Methods

2.1. Metabolomics Analysis

Phacellanthus tubiflorus (lot no. 2301, 2302, 2303) was supplied by the Changbai Mountain Academy of Sciences (Antu, Jilin, China). The sample was lyophilized using a freeze dryer (Scientz-100F) under vacuum conditions. The dried sample was then ground into powder using a grinder (MM400, Retsch) at 30 Hz for 1.5 minutes. A 50 mg portion of the powdered sample was weighed and extracted with 1200 μ L of 70% methanol pre-chilled to -20°C . The sample was vortexed every 30 minutes for 30 seconds, for a total of six times. After centrifugation (12,000 rpm for 3 minutes), the supernatant was collected and filtered through a 0.22 μ m pore size membrane. The filtered sample was then stored in injection vials for UPLC-MS/MS analysis.

Chromatographic separation was performed using an Agilent SB-C18 column (1.8 μ m, 2.1 mm \times 100 mm) maintained at 40°C . A 2 μ L sample volume was injected, and the flow rate was 0.35 mL/min. A binary solvent system was employed, consisting of mobile phase A (0.1% formic acid in ultrapure water) and mobile phase B (0.1% formic acid in acetonitrile). The following gradient elution program was used: 5% B for 0-9 min, a linear gradient to 95% B from 9-10 min, 5% B from 10-11.10 min, and a final linear gradient to 95% B from 11.10-14 min.

The electrospray ionization (ESI) source was operated at a temperature of 550°C . The ion spray voltage (IS) was set at 5500 V for positive ion mode and 1~4500 V for negative ion mode. Ion source gases I (GSI), II (GSII), and curtain gas (CUR) were set at 50, 60, and 25 psi, respectively. The collision-induced dissociation (CID) parameters were set to high. The triple quadrupole (QQQ) scan was performed in Multiple Reaction Monitoring (MRM) mode with nitrogen as the collision gas at a medium setting. The decluttering potential (DP) and collision energy (CE) for each MRM ion pair were optimized. MRM ion pairs were monitored according to the metabolites

eluted at each time point.

The data collection system mainly included an Ultra Performance Liquid Chromatography (UPLC) system (ExionLCM AD, <https://sciex.com.cn/>) and Tandem Mass Spectrometry (MS/MS).

2.2 Screening for shared Targets between *P. Tubiflorus* and AD

The compounds identified were searched for their Canonical SMILES numbers in the PubChem database (<https://pubchem.ncbi.nlm.nih.gov>). For compounds without available SMILES, their structures were drawn using ChemDraw and saved in SDF format, and the Canonical SMILES numbers were obtained through Open Babel. The SMILES numbers were uploaded to the Swiss Target Prediction database (<http://www.swisstargetprediction.ch>) to obtain potential targets, with a selection criterion of Probability > 0. Additionally, AD-related targets were retrieved from the GeneCards database (<https://www.genecards.org>). Venn diagrams were created using Venny (<http://www.liuxiaoyu.com>) to intersect the compound targets with AD targets, identifying the anti-Alzheimer's disease targets of *P. tubiflorus* active compounds.

2.3 PPI Network Analysis of Anti-Alzheimer's Disease Targets

The shared targets were imported into the STRING database (<http://www.string-db.org/>), selecting "Multiple Protein" and the species "Homo sapiens." A cutoff of $P < 0.05$ was used to filter the interactions, and a protein-protein interaction (PPI) network was constructed and visualized using Cytoscape 3.8.0 software.

2.4 GO and KEGG Enrichment Analysis

Gene Ontology (GO) and Kyoto Encyclopedia of Genes and Genomes (KEGG) pathway enrichment analyses were conducted using the DAVID database (<https://david.ncifcrf.gov/summary.jsp>), with a P-value cutoff of < 0.05 . Pathways unrelated to Alzheimer's disease, such as cancer pathways, were excluded from the analysis.

2.5 Active Ingredient-Target-Signaling Pathway Analysis

A network of "*P. tubiflorus* Active Ingredients-Targets" was constructed using Cytoscape 3.8.0 software to identify the main active ingredients

and important pathways in the anti-Alzheimer's effects of *P. tubiflorus* Active ingredients, targets, and pathways were represented as nodes, with edges indicating the interactions between active ingredients and targets.

2.6 Molecular Docking of Core Components and Key Targets

Molecular docking validation was performed for the potential active components of *P. tubiflorus* with key targets. The 3D structures of proteins were obtained by searching the PDB database (<https://www.rcsb.org/>) using the protein UniProt entry number. Chem 3D was used to optimize the main active compounds by energy minimization. The protein was preprocessed using PyMOL and Autodock software (removing water and ligands, adding charges, and preparing rotatable bonds). Molecular docking was performed using Autodock Vina, and docking results were visualized with PyMOL.

2.7 Cell Culture and Treatment

Human neuroblastoma SH-SY5Y cells were purchased from ATCC (Manassas, VA, USA; CRL-2266) and cultured in Dulbecco's modified Eagle's medium (DMEM, Gibco, 11995-065) with 10% fetal bovine serum (FBS, Gibco, 10082-147) and 1% penicillin-streptomycin solution (Gibco, 15140-122). Cells were maintained at 37 °C in a humidified atmosphere of 5% CO₂ and subcultured when reached 80-90% confluency.

Lyophilized A β ₁₋₄₂ powder purchased from Cellmano Biotech (Hefei, China) was processed with HFIP and dissolved in DMSO to a final concentration of 5 mM, followed by sonication in a water bath for 10 minutes to ensure complete suspension. The monomeric aliquot was then diluted with sterile phosphate-buffered saline (PBS) to a final concentration of 100 μ M, vortexed for 30 seconds, and incubated for 24 hours at 4°C to obtain oligomeric A β ₁₋₄₂.

SH-SY5Y cells were seeded into 48-well plates at a density of 2×10^5 cells/mL and incubated for 24 h. Subsequently, the cells were treated with *P. Tubiflorus* (25, 50, 100 μ g/ml), or aggregated A β ₁₋₄₂ (10 μ M), or a combination of *P. tubiflorus* (25, 50, 100 μ g/ml) and aggregated A β ₁₋₄₂ (10 μ M) for additional 24 h. Cells viability and cytotoxicity were measured by MTT and LDH assays (G4000, J2380, Promega Beijing, Co., Ltd.), respectively, according to manufacturer's

instructions. Absorbance measurements were obtained using a microplate spectrophotometer (I-mark, Bio-Rad, Hercules, CA, USA).

2.8 ELISA Assay

SH-SY5Y cells were treated with aggregated A β (10 μ M) alone or without aggregated A β for 6 h and then replace with conditioned medium containing *P. t.* (0, 25, 50, and 100 μ g/ml) and incubated at 37 °C for 24 h. The medium was collected respectively and the secretions of TNF α , IL-1 β , and IL-6 were measured by commercially available kits (ELH-TNF α , ELH-IL1b, and ELH-IL6, RayBiotech Life, Inc., GA, USA) according to the manufacturer's instructions.

2.9 Antibody Array Assay

SH-SY5Y cells were treated with aggregated A β (10 μ M) for 6 h and then replaced with conditioned medium containing 100 μ g/ml *P. tubiflorus* for 24h. Cells were washed with prewarmed PBS and subjected to array assays according to manufacturer's instructions (AAH-JAKSTAT-1, AAH-AKT-1, RayBiotech Life, Inc., GA, USA).

2.10 Statistical Analysis

The molecular ion peaks, MS/MS fragmentation patterns, and characteristic fragments of each component were analyzed using Analyst 1.6.3 software. Compound structures were identified based on data from the PubChem database and related literature reports. Statistical analyses were performed using Prism software (GraphPad 9). Direct comparisons within single genotype groups were conducted using one-way ANOVA followed by Tukey's post hoc test or Student's t-test. Statistical significance was defined as * $p < 0.05$, ** $p < 0.01$, and *** $p < 0.001$. All experiments were performed independently at least three times, with results expressed as the mean \pm standard error of the mean (SEM).

3. Results

3.1 Chemical Composition of *P. tubiflorus*

The chemical composition of *P. tubiflorus* was systematically analyzed by UPLC-Q-TOF/MS in both positive and negative ion modes. The total ion chromatograms (TICs) are shown in Figure 1. A total of 1,536 compounds were identified and the top 10 with relatively high abundance were selected based on relevant literature. Detailed results are presented in Table 1.

Table 1 The identification of chemical constituents from *P. tubiflorus*

NO.	Relative content (area)	Molecular formula	Molecular ion (m/z)	Characteristic ion (m/z)	Compound
1	1.31*10 ⁸	C ₂₉ H ₃₆ O ₁₅	623.2	161.02	Magnoloside D
2	1.16*10 ⁸	C ₂₉ H ₃₆ O ₁₅	623.2	461.17	Acteoside
3	4.79*10 ⁷	C ₁₁ H ₁₅ N ₅ O ₃ S	298.1	136.06	5'-Deoxy-5'-(methylthio) adenosine
4	4.70*10 ⁷	C ₈ H ₁₈ N ₂ O ₂	175.12	70.07	N(6), N(6)-Dimethyl-L-lysine
5	4.01*10 ⁷	C ₁₇ H ₂₄ O ₁₁	403.12	121.03	Kingiside
6	3.74*10 ⁷	C ₂₈ H ₃₈ O ₁₄	597.22	375.14	Picraquassioside C
7	3.61*10 ⁷	C ₁₃ H ₁₆ O ₈	299.72	137.0244	Salicylic acid-2-O-glucoside
8	3.44*10 ⁷	C ₁₀ H ₁₃ N ₅ O ₃	252.11	136.06	Cordycepin
9	3.41*10 ⁷	C ₂₁ H ₃₀ O ₉	427.19	265.14	Pterosin L 2'-O-Beta-D-Glucoside
10	3.37*10 ⁷	C ₂₀ H ₂₆ O ₁₀	427.16	265.11	Hydroxyrudicoumarin C glucoside

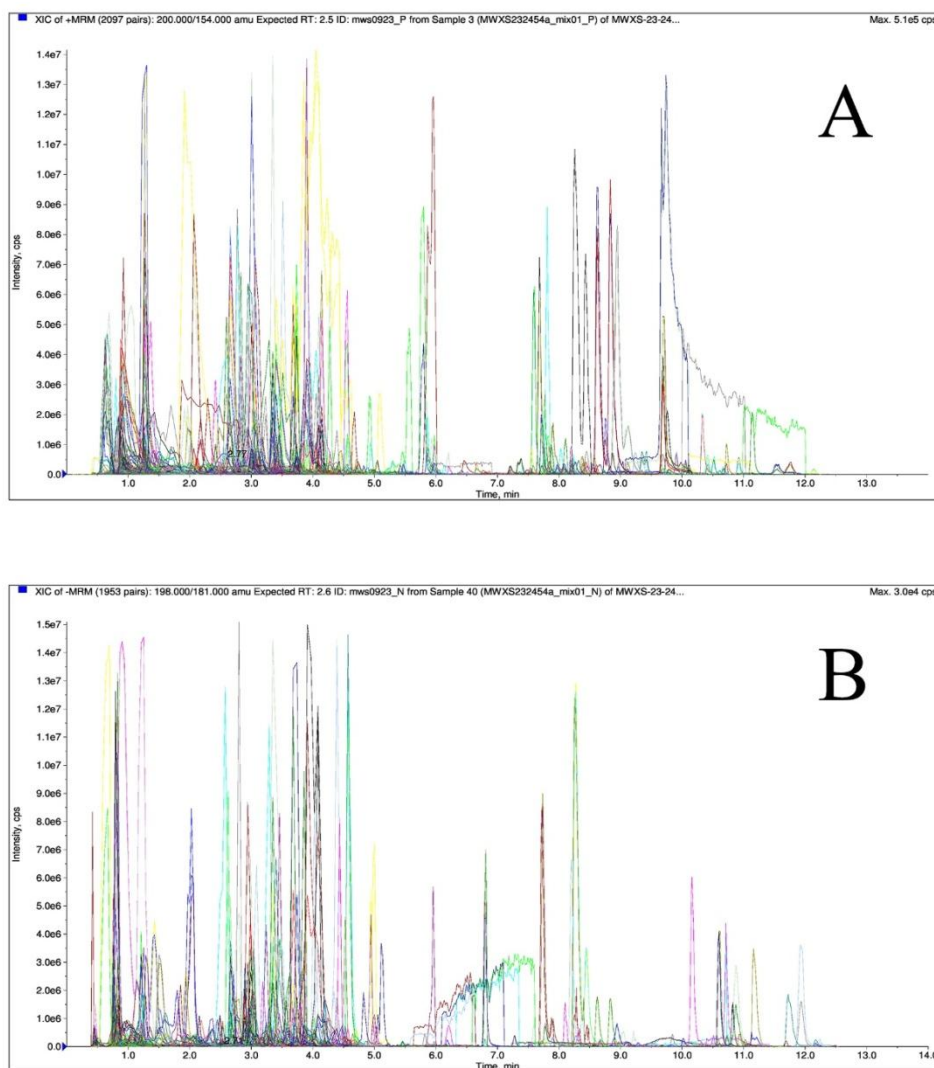


Figure 1 Total ion chromatogram of *P. tubiflorus* in positive(A) and negative(B) ion mode.

3.2 Prediction of Active Ingredient Targets

Using the Swiss Target Prediction database, a total of 477 genes were identified. After filtering the duplicated genes, 282 putative target genes of 10 compounds were obtained. Following that,

15726 genes linked to AD were retrieved from the GeneCards database. A Venn diagram was constructed to anticipate the shared targets (Figure 2). A total of 269 potential targets of *P. tubiflorus* that protect against AD were chosen and regarded as hub targets.

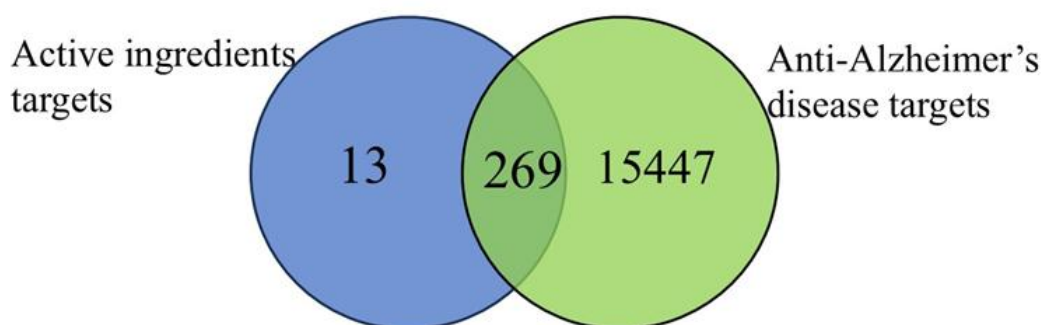


Figure 2 Venn diagram of anti- AD targets and active ingredients.

3.3 PPI Interaction Network Construction

A protein-protein interaction (PPI) network of gene lists was constructed using the STRING database (v12.0) and visualized by Cytoscape (v3.10.1) (Figure 3). The network contains 257

nodes and 7,546 edges, with an average node degree of 29.362 and an average betweenness centrality of 0.526. The top 10 core genes (SRC, TNF, AKT1, IL1B, IL6, TP53, EGFR, NT5E, ESR1, and PRKACA) were identified using the Cytoscape plugin CytoHubba.

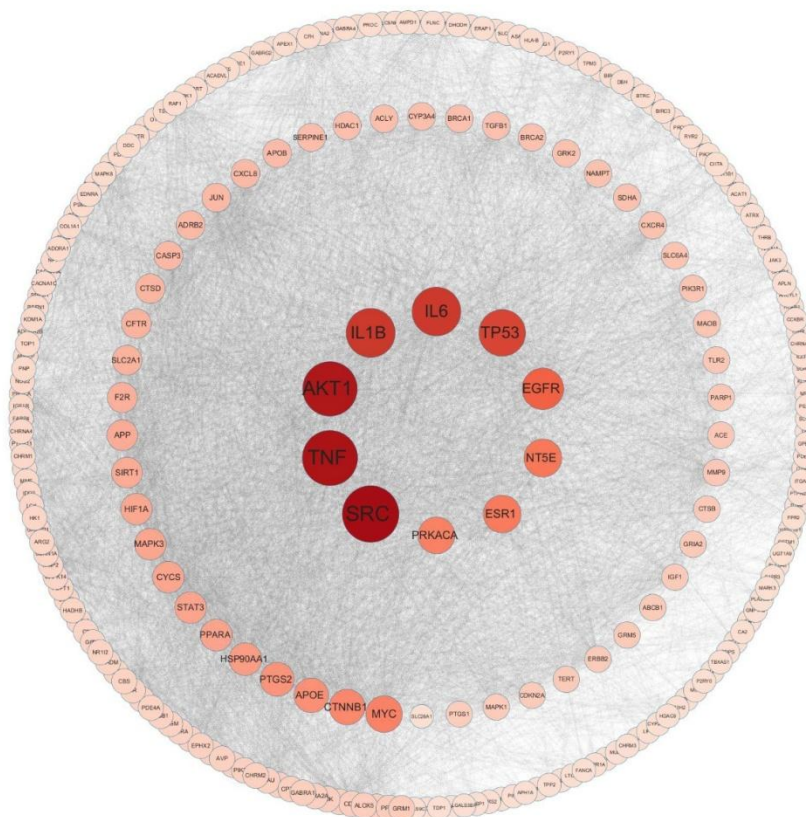


Figure 3 PPI network diagram of protein targets.

3.4 Enrichment Analysis

To explore the biological processes involved in the anti-AD effects of *P. tubiflorus*, 269 overlapping target genes were imported into the DAVID database for GO and KEGG enrichment analyses. The GO analysis identified 265 significant biological functions, including 167 biological processes (BP), 37 cellular components (CC), and 61 molecular functions (MF). The top 10 results in each category were plotted as bubble charts (Figure 4A). In biological processes, response to xenobiotic stimulus, positive regulation of gene expression, and response to hypoxia accounted for the majority. The plasma

membrane, neuronal cell body, and extracellular exosome dominated the enriched CC ontologies. Molecular functions were primarily dominated by enzyme binding, protein binding, and identical protein binding.

KEGG pathway enrichment analysis of 269 targeted genes revealed 72 potential signaling pathways. The top-ranking pathways were visualized in circular plots (Figure 4B). The results showed that most relevant enriched signaling pathway are the neuroactive ligand-receptor interaction and cAMP signaling pathways.

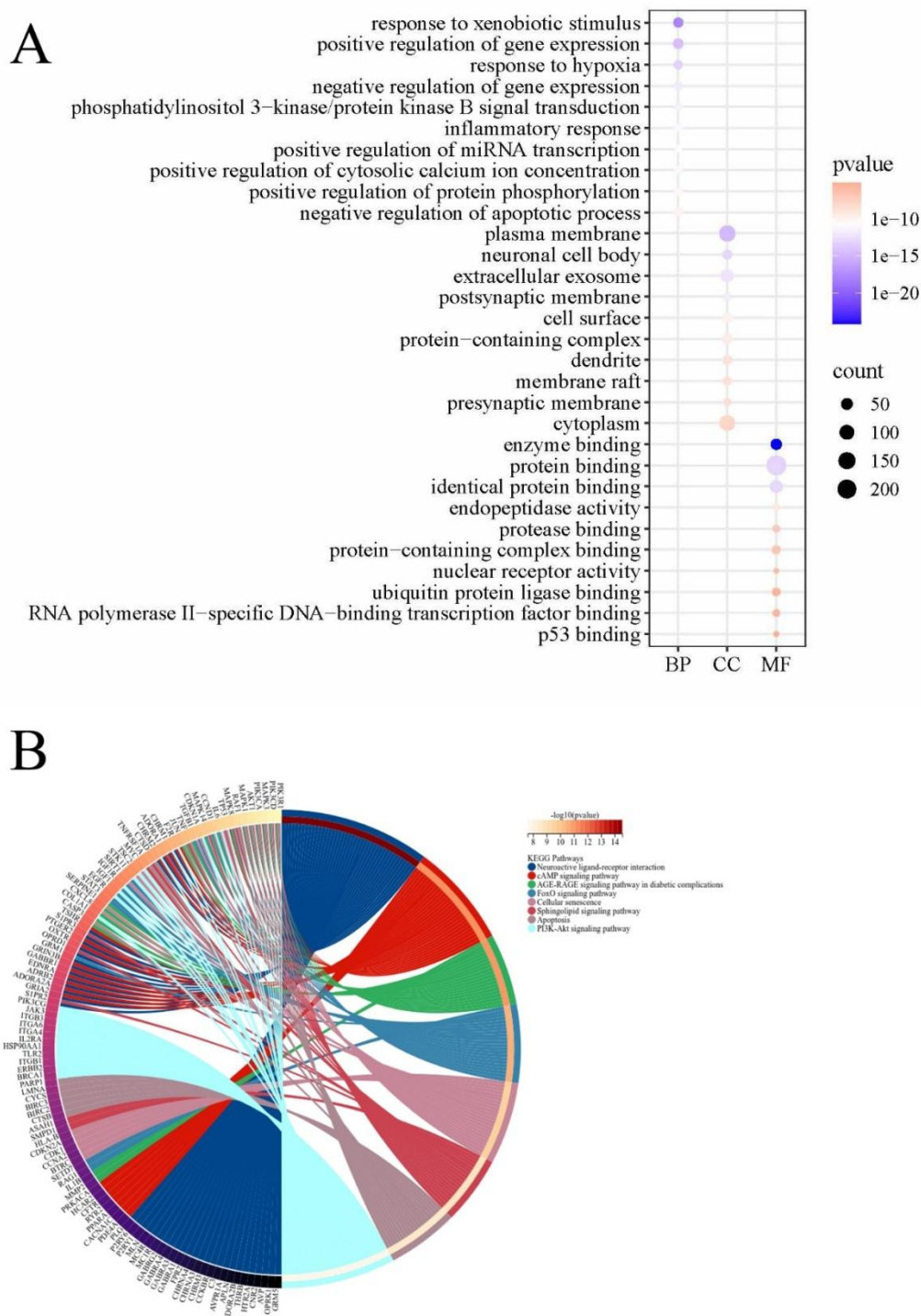


Fig. 4 Enrichment analysis plot. (A) Gene Ontology enrichment analysis. (B) Kyoto Encyclopedia of Genes and Genomes pathway enrichment analysis.

3.5 Molecular Docking Validation

The 10 core compounds (Magnolioside D (MGD), Acteoside (ACT), 5'-Deoxy-5'-(methylthio) adenosine (ADE), N(6), N(6)-Dimethyl-L-lysine (6NN), Kingiside (KGS), Picraquassioside C (PIC), Salicylic acid-2-O-glucoside (SAG), Cordycepin (CDP), Pterosin L 2'-O-Beta-D-Glucoside (PODG), and Calceolarioside A (CCL)) were docked with 5 key targets (SRC, TNF,

AKT1, IL1B, and IL6) for validation. The binding affinity between protein and compound was represented by the binding energy. Generally, a binding energy below -5.0 kcal/mol suggests good binding affinity, while values below -7.0 kcal/mol indicate a strong interaction. The functional groups involved in docking were primarily carboxyl, hydroxyl, and ester groups on the respective carbon chains. For the most effective

binding affinity (Table 2), they are SRC-MGD (-9.7 kcal/mol), TNF-ACT (-9.7 kcal/mol), TNF-PODG (-10.3 kcal/mol), AKT1-MGD (-7.5 kcal/mol), IL1B-MGD (-7.5 kcal/mol) and IL6-CCL (-7.6 kcal/mol). Visualization was conducted

using PyMOL software and results were shown in Figure 5. According to the docking results, we applied Magnoloside D for the subsequent *in vitro* validation tests.

Table 2 Docking energy of the complex between core compounds and key targets

Compound	Binding energy (kcal/mol)				
	SRC	TNF	AKT1	IL1B	IL6
Magnoloside D	-9.7	-9.3	-7.5	-7.5	-7.5
Acteoside	-9.2	-9.7	-7.2	-7.2	-6.9
5'-Deoxy-5'-(methylthio)adenosine	-6.9	-6.9	-5.3	-5.9	-5.5
N(6),N(6)-Dimethyl-L-lysine	-5.5	-5.7	-4.2	-4.4	-4.9
Kingiside	-7.7	-5.0	-6.0	-6.4	-6.7
Picraquassioside C	-8.1	-8.0	-7.0	-7.0	-6.3
Salicylic acid-2-O-glucoside	-7.0	-7.3	-6.3	-5.8	-5.9
Cordycepin (3'-Deoxyadenosine)	-6.7	-7.3	-5.2	-5.8	-5.9
Pterosin L 2'-O-Beta-D-Glucoside	-9.4	-10.3	-7.2	-7.4	-7.1
Calceolarioside A	-8.9	-9.2	-6.8	-7.0	-7.6

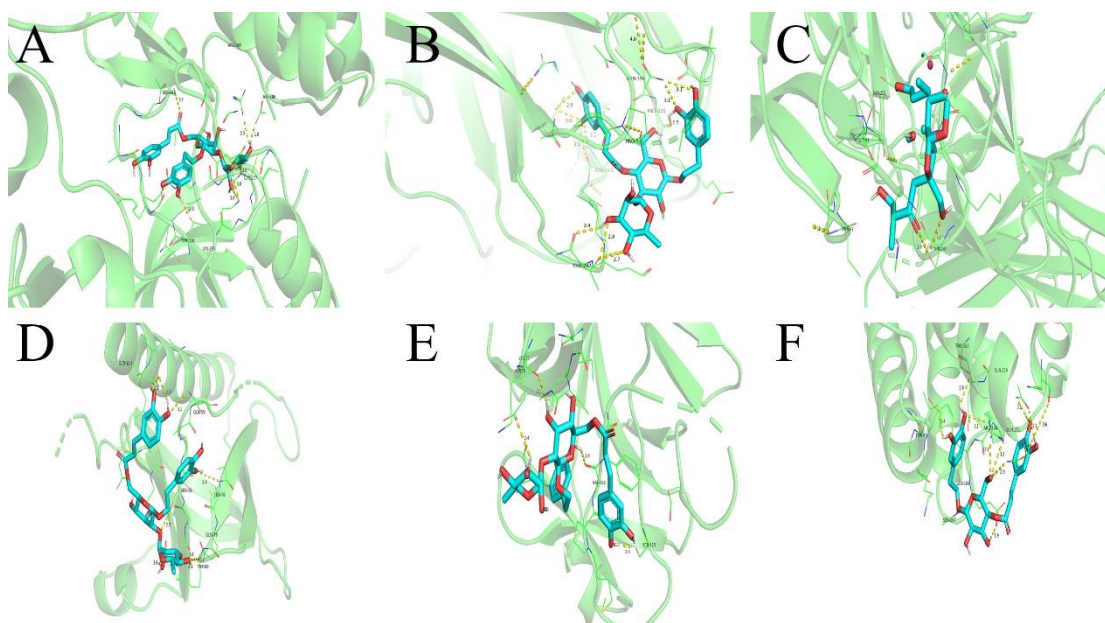


Fig. 5 Molecular docking results between core components and pivotal targets. A:SRC-MGD; B: TNF-ACT; C: TNF-PODG; D: AKT1-MGD; E: IL1B-MGD; F: IL6-CCL.

3.6 Validations of the protective effects of Magnoloside D on AD *in vitro*

To verify the neuroprotective effects of *P. tubiflorus* against $A\beta_{1-42}$ -induced cytotoxicity, cell viability and cytotoxicity were assessed in SH-SY5Y cells following treatment with $A\beta_{1-42}$, both

in the presence and absence of Magnoloside D (10, 20, 40 $\mu\text{g/ml}$). Magnoloside D significantly restored cell viability in a concentration-dependent manner, as evidenced by an approximate 29% increase at the 20 $\mu\text{g/ml}$ compared to the $A\beta_{1-42}$ -treated group (Fig. 6A). Concurrently, Magnoloside D (10, 20, 40 $\mu\text{g/ml}$)

mitigated the toxicity induced by aggregated $A\beta_{1-42}$ in neuronal cells, with the lowest LDH release observed in the group of 20 $\mu\text{g/ml}$ of Magnoloside D (Figure 6A). These findings indicated that

Magnoloside D exerted a significant protective effect against $A\beta_{1-42}$ -induced cytotoxicity in neuronal cells.

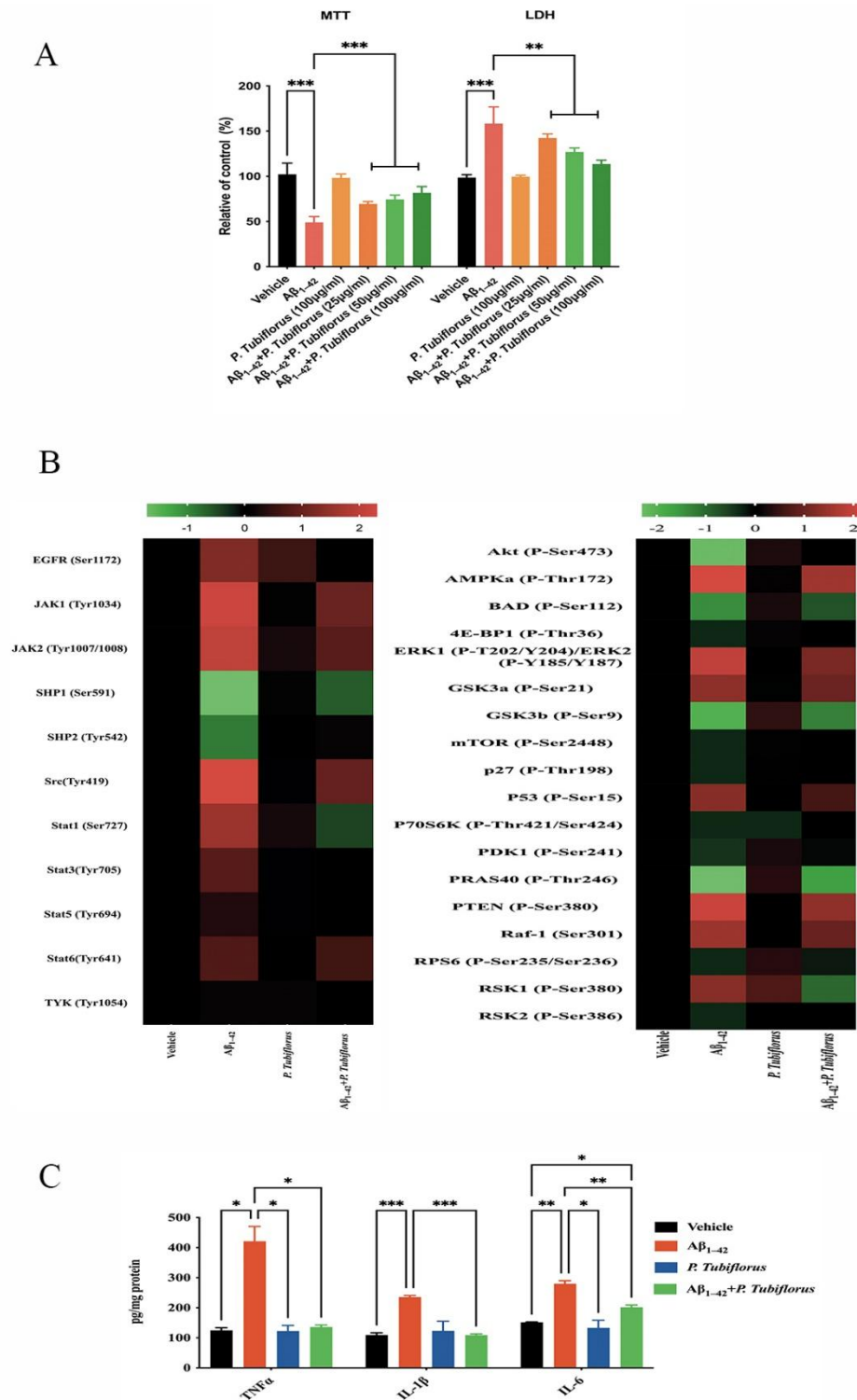


Figure 6 Magnoloside D protects cells from aggregated amyloid β ($A\beta$)-induced toxicity in vitro. (A) Cell viability and cytotoxicity were assessed using MTT and LDH assays, respectively. (B) Heatmaps of human JAK/STAT pathway and AKT pathway phosphorylation arrays. Fold changes are denoted in red for upregulation and green for downregulation. (C) ELISA assays of $\text{TNF}\alpha$, $\text{IL-1}\beta$, and IL-6 . All experiments were performed in triplicate, and data are mean \pm SEM. * $p < 0.05$, ** $p < 0.01$, and *** $p < 0.001$.

The modulatory effects of Magnolioside D on SRC and AKT were evaluated using the post-translational modification arrays. Consisted with the molecular docking predictions, Magnolioside D significantly downregulated SRC (2.77-fold decrease) and upregulated AKT (2.36-fold increase) in SH-SY5Y cells exposed to A β ₁₋₄₂ (Fig.6B). Concomitantly, the secretions of inflammatory factors TNF α , IL-1 β , and IL-6 were markedly inhibited by Magnolioside D (Fig.6C). These findings suggest that Magnolioside D confers neuroprotection against A β ₁₋₄₂-induced injury, at least in part, via modulation of the predicted target genes.

4. Discussion

Alzheimer's disease is marked by the accumulation of amyloid-beta plaques and tangled tau proteins in the brain, ultimately triggering neuroinflammation and disrupting synaptic function^[14, 15]. Intriguingly, early findings suggest that specific plant-based compounds may offer a way to influence these core disease processes, potentially by reducing inflammation, combating oxidative stress, and interfering with amyloid formation^[16, 17]. This warrants thorough scientific exploration to determine their effectiveness in slowing AD progression. Within the theoretical framework of Traditional Chinese Medicine (TCM), the administration of nephrotonic herbal remedies is posited to exert salutary effects on cerebral function, thereby presenting potential therapeutic strategies for neurological pathologies. This tenet is rooted in the TCM understanding of the kidney's role in governing 'jing' (essence) and its subsequent influence on the generation of marrow, which is considered to nourish the brain. Consequently, interventions aimed at augmenting renal function are theorized to positively modulate cognitive processes and potentially attenuate the progression of neurodegenerative disorders. In this study, the chemical components of *P. tubiflorus* were first characterized using UPLC-MS technology and confirmed 10 relative abundant compounds such as Magnolioside D (MGD), Acteoside (ACT), Pterosin L 2'-O-Beta-D-Glucoside (PODG), and Calceolarioside A (CCL). Ten hub genes of *P. tubiflorus* and AD, such as SRC, TNF, AKT1, IL1B, and IL6, and signaling pathways such as neuroactive ligand-receptor interaction and cAMP, were selected via Network pharmacology analyses. These hub genes

and pathways are important regulators and play a pivotal role in elucidating underlying pharmacological mechanisms by which *P. tubiflorus* exerts anti-AD effects.

In this study, KEGG pathway enrichment analysis, highlighting seven pathways significantly impacted by genes shared between *P. tubiflorus* and Alzheimer's disease (AD), directly informed the selection of SRC, TNF, AKT1, IL1B, and IL6 for validation. Specifically, AKT1 is central to the PI3K-Akt pathway and involved in cAMP^[18], FoxO^[17], apoptosis^[19], and AGE-RAGE signaling^[20]. TNF, within neuroactive ligand-receptor interaction, activates PI3K-Akt^[21] and the production of pro-inflammatory cytokines IL1B and IL6^[22], crucial in the AGE-RAGE pathway^[23]. SRC, participating in neuroactive ligand-receptor interactions, modulates PI3K-Akt^[24] and FoxO signaling^[25], impacting cellular senescence^[26]. These genes represent key biological processes dysregulated in AD, including inflammation (TNF, IL1B, IL6), cell survival and apoptosis (AKT1, SRC), and signal transduction (SRC, AKT1, TNF). Therefore, validating the effects of *P. tubiflorus* on these genes will provide critical mechanistic insights into its potential therapeutic action against AD's multifaceted pathology by modulating these interconnected pathways.

To validate the predictions, molecular dockings were further employed and binding energy data revealed varying affinities of the ten compounds for the selected target genes relevant to Alzheimer's Disease (AD) treatment. Notably, Magnolioside D and Pterosin L 2'-O-Beta-D-Glucoside exhibit the strongest binding across multiple targets, suggesting a higher potential for interaction and modulation of these proteins. Pterosin L 2'-O-Beta-D-Glucoside shows particularly high affinity for TNF, while Magnolioside D also demonstrates strong binding to SRC and TNF. Conversely, compounds like N(6), N(6)-Dimethyl-L-lysine and 5'-Deoxy-5'-(methylthio) adenosine show considerably weaker binding across all targets. These *in silico* docking studies suggest Magnolioside D, a compound isolated from *P. tubiflorus*, as a potential therapeutic agent for AD.

These *in silico* findings promoted further investigation *in vitro*. Critically, *in vitro* experiments validated this prediction.

Magnoloside D significantly restored the cell viability and reduced the LDH release in the model, highlighting the neuroprotective effects. The post-translational modification arrays indicated that SRC and AKT1 phosphorylation were remarkably impacted by Magnoloside D. SRC is implicated in multiple aspects of AD pathology, primarily through its ability to phosphorylate tyrosine residues on target proteins. Dysregulation of SRC activity, potentially could contribute to A β production, tau hyperphosphorylation, synaptic dysfunction, and neuroinflammation [27, 28]. Unlike SRC, which primarily focuses on tyrosine phosphorylation, AKT1's serine/threonine kinase activity impacts a different set of downstream targets and cellular processes, contributing to neuronal dysfunction and vulnerability [29, 30]. This reduction is likely influenced by and contributes to the altered levels and activity of SRC and the pro-inflammatory cytokines TNF, IL-1B, and IL-6 [31]. This complex interplay contributes to the pathological cascade of AD, highlighting the importance of these molecules as potential therapeutic targets. Additionally, other proteins in these two arrays are intricately linked and play important roles in neuroinflammation. ELISA assays indicated significant suppression of TNF α , IL-1B, and IL-6 by *P. tubiflorus*. Collectively, this study suggested that Magnoloside D could mitigate AD by regulating SRC, AKT1, TNF, IL-1B, and IL-6.

In summary, this study employed metabolic analysis, network pharmacology, molecular docking, and in vitro neuronal cell validation to delineate the potentials and mechanisms of *P. tubiflorus* in AD treatment. We identified the pivotal bioactive compound Magnoloside D and predicted its putative interactions with the core targets genes and signaling pathways implicated in the disease's pathology. Importantly, these findings highlighted *P. tubiflorus* as a competent therapeutic candidate that could modulate neuroinflammation, a critical driver in neurodegenerative disorders.

Fundings: This work was supported by National Key Research and Development Program of China (2023YFD2201802) and 5·5 Engineering Research & Innovation Team Project of Beijing Forestry University (BLRC2023A01).

CRedit Authorship Contribution Statement

Cheng Chang: Writing-original draft.

Declaration of Competing Interest

The authors declare no conflicts of interests.

Data Availability

Data available on request

References

1. Misiura, M. B., Butts, B., Hammerschlag, B., Munkombwe, C., Bird, A., Fyffe, M., Hemphill, A., Dotson, V. M. and Wharton, W., Intersectionality in Alzheimer's Disease: The Role of Female Sex and Black American Race in the Development and Prevalence of Alzheimer's Disease. *Neurotherapeutics*, 2023, 20, 1019-1036.
2. Kamatham, P. T., Shukla, R., Khatri, D. K. and Vora, L. K., Pathogenesis, diagnostics, and therapeutics for Alzheimer's disease: Breaking the memory barrier. *Ageing Research Reviews*, 2024, 101, 102481.
3. Wang, H., Yan, Z., Yang, W., Liu, R., Fan, G., Gu, Z. and Tang, Z., A strategy of monitoring acetylcholinesterase and screening of natural inhibitors from *Uncaria* for Alzheimer's disease therapy based on near-infrared fluorescence probe. *Sensors and Actuators B: Chemical*, 2025, 424, 136895.
4. Shankar, G., Kumar, P., Rai, S., Ghosh, A., Varma, T., Wani, M. A., Kumar, S., Mandloi, U., Singh, G. K., Garg, P., Kulkarni, O., Srikrishna, S., Kumar, S. and Modi, G., Discovery of novel hybrid tryptamine-rivastigmine molecules as potent AChE and BChE inhibitors exhibiting multifunctional properties for the management of Alzheimer's disease. *European Journal of Medicinal Chemistry*, 2025, 283, 117066.
5. Gajendra, K., Pratap, G. K., Poornima, D. V., Shantaram, M. and Ranjita, G., Natural acetylcholinesterase inhibitors: A multi-targeted therapeutic potential in Alzheimer's disease. *European Journal of Medicinal Chemistry Reports*, 2024, 11, 100154.
6. Pandey, S. N., Rangra, N. K., Singh, S., Arora, S. and Gupta, V., Evolving Role of Natural Products from Traditional Medicinal Herbs in the Treatment of Alzheimer's Disease. *ACS Chemical Neuroscience*, 2021, 12, 2718-2728.
7. Singh, A., Agarwal, S. and Singh, S., Age related neurodegenerative Alzheimer's disease: Usage of traditional herbs in

- therapeutics. *Neuroscience Letters*, 2020, 717, 134679.
8. Koppula, S., Wankhede, N. L., Sammeta, S. S., Shende, P. V., Pawar, R. S., Chimthanawala, N., Umare, M. D., Taksande, B. G., Upaganlawar, A. B., Umekar, M. J., Kopalli, S. R. and Kale, M. B., Modulation of cholesterol metabolism with Phytoremedies in Alzheimer's disease: A comprehensive review. *Ageing Research Reviews*, 2024, 99, 102389.
 9. Xu, X., Wang, L., Zhang, K., Zhang, Y. and Fan, G., Managing metabolic diseases: The roles and therapeutic prospects of herb-derived polysaccharides. *Biomedicine & Pharmacotherapy*, 2023, 161, 114538.
 10. Xu, T., Yin, J., Dai, X., Liu, T., Shi, H., Zhang, Y., Wang, S., Yue, G., Zhang, Y., Zhao, D., Gao, S., Prentki, M., Wang, L. and Zhang, D., Cnidii Fructus: A traditional Chinese medicine herb and source of antiosteoporotic drugs. *Phytomedicine*, 2024, 128, 155375.
 11. Xu, G., Zhang, X., Yin, L. and Bai, Y., Phacellanthus tubiflorus. *Journal of Plant*, 1991, 48+50(in chinese).
 12. Akki, A. J., Patil, S. A., Hungund, S., Sahana, R., Patil, M. M., Kulkarni, R. V., Raghava Reddy, K., Zameer, F. and Raghu, A. V., Advances in Parkinson's disease research – A computational network pharmacological approach. *International Immunopharmacology*, 2024, 139, 112758.
 13. Wang, X., Wang, Y., Yuan, T., Wang, H., Zeng, Z., Tian, L., Cui, L., Guo, J. and Chen, Y., Network pharmacology provides new insights into the mechanism of traditional Chinese medicine and natural products used to treat pulmonary hypertension. *Phytomedicine*, 2024, 135, 156062.
 14. Kiraly, M., Foss, J. F. and Giordano, T., Neuroinflammation, Its Role in Alzheimer's Disease and Therapeutic Strategies. *The Journal of Prevention of Alzheimer's Disease*, 2023, 10, 686-698.
 15. Cheng, Q., Fan, Y., Zhang, P., Liu, H., Han, J., Yu, Q., Wang, X., Wu, S. and Lu, Z., Biomarkers of Synaptic Degeneration in Alzheimer's Disease. *Ageing Research Reviews*, 2024, 102642.
 16. Hossain, M. S., Das, A., Rafiq, A., Deák, F., Bagi, Z., Outlaw, R., Varadarajan, S., Yamamoto, M., Kaplan, J. H., Ushio-Fukai, M. and Fukai, T., Novel Role of Copper Transport Proteins in Oxidative Stress-Dependent Brain Endothelial Barrier Dysfunction and Inflammation Associated with Alzheimer's Disease. *Free Radical Biology and Medicine*, 2024, 224, S24.
 17. Dash, U. C., Swain, S. K., Kanhar, S., Banjare, P., Roy, P. P., Dandapat, J. and Sahoo, A. K., The modulatory role of prime identified compounds in *Geophila repens* in mitigating scopolamine-induced neurotoxicity in experimental rats of Alzheimer's disease via attenuation of cholinesterase, β -secretase, MAPt levels and inhibition of oxidative stress imparts inflammation. *Journal of Ethnopharmacology*, 2022, 282, 114637.
 18. Guo, N., Wang, X., Xu, M., Bai, J., Yu, H. and Le, Z., PI3K/AKT signaling pathway: Molecular mechanisms and therapeutic potential in depression. *Pharmacological Research*, 2024, 206, 107300.
 19. Kim, I. Y., Song, S. H., Seong, E. Y., Lee, D. W., Bae, S. S. and Lee, S. B., Akt1 is involved in renal fibrosis and tubular apoptosis in a murine model of acute kidney injury-to-chronic kidney disease transition. *Experimental Cell Research*, 2023, 424, 113509.
 20. You, X.-L., Zhao, M.-L., Liu, Y.-R., Tang, Z.-S., Zhao, Y.-T., Yan, L. and Song, Z.-X., *Hypericum perforatum* L. protects against renal function decline in ovariectomy rat model by regulating expressions of NOS3 and AKT1 in AGE-RAGE pathway. *Phytomedicine*, 2024, 123, 155160.
 21. Fahmy, M. I., Khalaf, S. S. and Elrayess, R. A., The neuroprotective effects of alpha lipoic acid in rotenone-induced Parkinson's disease in mice via activating PI3K/AKT pathway and antagonizing related inflammatory cascades. *European Journal of Pharmacology*, 2024, 980, 176878.
 22. Tian, X., Wang, W.-T., Zhang, M.-M., Yang, Q.-Q., Xu, Y.-L., Wu, J.-B., Xie, X.-X., Wang, J.-Y. and Wang, J.-Y., Red nucleus mGluR1 and mGluR5 facilitate the development of neuropathic pain through stimulating the expressions of TNF- α and IL-1 β . *Neurochemistry International*, 2024, 178, 105786.
 23. Zhang, D., Qin, H., Chen, W., Xiang, J., Jiang, M., Zhang, L., Zhou, K. and Hu, Y., Utilizing network pharmacology, molecular docking,

- and animal models to explore the therapeutic potential of the WenYang FuYuan recipe for cerebral ischemia-reperfusion injury through AGE-RAGE and NF- κ B/p38MAPK signaling pathway modulation. *Experimental Gerontology*, 2024, 191, 112448.
24. Cui, Q.-L., Fogle, E. and Almazan, G., Muscarinic acetylcholine receptors mediate oligodendrocyte progenitor survival through Src-like tyrosine kinases and PI3K/Akt pathways. *Neurochemistry International*, 2006, 48, 383-393.
25. Bülow, M. H., Bülow, T. R., Hoch, M., Pankratz, M. J. and Jünger, M. A., Src tyrosine kinase signaling antagonizes nuclear localization of FOXO and inhibits its transcription factor activity. *Sci Rep*, 2014, 4, 4048.
26. Aneurillas, C., Herman, A. B., Rossi, M., Munk, R., Lehrmann, E., Martindale, J. L., Cui, C. Y., Abdelmohsen, K., De, S. and Gorospe, M., Early SRC activation skews cell fate from apoptosis to senescence. *Sci Adv*, 2022, 8, eabm0756.
27. Meur, S. and Karati, D., Fyn Kinase in Alzheimer's Disease: Unraveling Molecular Mechanisms and Therapeutic Implications. *Mol Neurobiol*, 2024.
28. Portugal, C. C., Almeida, T. O., Socodato, R. and Relvas, J. B., Src family kinases (SFKs): critical regulators of microglial homeostatic functions and neurodegeneration in Parkinson's and Alzheimer's diseases. *Febs j*, 2022, 289, 7760-7775.
29. Wang, Y., Ye, X., Su, W., Yan, C., Pan, H., Wang, X. and Shao, S., Diosmin ameliorates inflammation, apoptosis and activates PI3K/AKT pathway in Alzheimer's disease rats. *Metab Brain Dis*, 2024, 39, 1405-1415.
30. Lu, L., Fu, Z., Wu, B., Zhang, D. and Wang, Y., Leptin ameliorates A β 1-42-induced Alzheimer's disease by suppressing inflammation via activating p-Akt signaling pathway. *Transl Neurosci*, 2023, 14, 20220270.
31. Yang, W., Liu, Y., Xu, Q. Q., Xian, Y. F. and Lin, Z. X., Sulforaphene Ameliorates Neuroinflammation and Hyperphosphorylated Tau Protein via Regulating the PI3K/Akt/GSK-3 β Pathway in Experimental Models of Alzheimer's Disease. *Oxid Med Cell Longev*, 2020, 2020, 4754195.